Chemical Physics 22 (1977) 1–12

EXCITON BAND OF A ONE-MOLECULE-PER-UNIT-CELL CRYSTAL: HEXAMETHYLBENZENE FIRST SINGLET*

S.D. WOODRUFF and R. KOPELMAN
Department of Chemistry, The University of Michigan, Ann Arbor, Michigan 48109, USA

Received 7 January 1977

The exciton band structure has been determined experimentally, from quantitative band–band fluorescence and absorption measurements, for the first singlet excited state of the low temperature phase of the hexamethylbenzene crystal. At 2 K, the center of the band is at 35156 cm^{-1}, its bottom (the $\kappa = 0$ state) at 35134 cm^{-1} and its total extent about 40 cm^{-1} (i.e. much larger than anticipated earlier). We derive a dispersion relation, based on the trigonal topology of the crystal, with six out-of-plane nearest neighbor pairwise interactions of -3.3 cm^{-1} and six in-plane ones of -0.4 cm^{-1}. These parameters, based on the exciton band shape, are *inconsistent* with a transition-multipole–transition-multipole model, and in particular with an octopole–octopole one, based on the π electrons. π–σ interactions are suggested. The neat crystal data are fully consistent with a complete concentration study on isotopic mixed samples of hexamethylbenzene, at 2 K, by absorption and fluorescence spectra with a 1 cm^{-1} resolution. The mixed crystal results are also consistent with the energy and spectral moments given by the separated-band model and with the behaviour expected from cluster percolation and exciton percolation.

1. Introduction

The investigation of the exciton bands of the excited states of molecules in crystals is of importance because the exciton band is a direct result of the perturbations of the crystal environment on the excited states of the molecules. In the case of organic molecular crystals where the molecules remain as discrete units in the crystal and the electrons remain tightly bound to the parent molecules in the lower excited (non-conducting) states, the crystals are said to be in the Frenkel tight binding limit. Thus far only two other molecular crystals, benzene and naphthalene, have had the exciton band density of states of one of their excited singlet states determined experimentally [1,2]. We notice that only "spin allowed" excitons (i.e., singlet excitons) can give direct information on the Coulomb-type excitation exchange interactions [1,3].

Benzene and naphthalene have four and two molecules per unit cell, respectively, in their crystalline forms, thus giving rise to an interchange symmetry [3] which must be considered in understanding the effects of the crystal lattice on the molecule. Hexamethylbenzene (HMB) however, has but one molecule per unit cell in its low temperature phase III form [4] and as such has a trivial C_1 interchange group. Thus the Frenkel exciton theory gives an exact, symmetry based, solution for HMB, unlike the situation for benzene and naphthalene [1,3]. There are some other factors which make HMB a suitable candidate for this study. First, the molecule is similar to benzene, especially if the methyl groups are assumed to be "amorphous" units, and thus much of the electronic and vibrational spectra can be correlated to benzene. Second, the crystal site symmetry of HMB in phase III has been determined to be S_6 and thus the crystal structure is trigonal for that phase [4]. The orientation of the molecule in the S_6 site enables easy differentiation between the kinds of pairwise interactions which must be accounted for in the exciton band study, and also indicates a complex topology of interactions which actually smoothes

* Supported by NSF Grant DMR75-07832 A01 and NIH Grant NS08116-08.

the appearance of the isotopic mixed crystal spectra of HMB.

In this paper the results of the experimental determination of the exciton band density of states of the first excited singlet state of HMB will be presented. These results will be compared to calculations of the density of states, using the general Frenkel exciton model, and pairwise intermolecular interactions for the first excited singlet state will be assigned. An exciton dispersion relation is given, which is consistent with both the "neat" and the isotopic mixed crystal data including energy transfer.

2. Experimental

The HMB obtained from Aldrich was purified by recrystallization from hot ethanol. The perdeuterohexamethylbenzene (HMB-d_{18}) obtained from Merck, Sharp, and Dohme with the quoted purity of 99% atom deuterium was used without further purification. Thin (10–100 μ) neat and isotopic mixed crystals of HMB and HMB-d_{18} were grown from benzene solution over water. Large (1–5 mm) crystals of neat HMB were grown from the melt by the Bridgman technique. Sample temperatures of 2 K and 77 K were obtained by immersing the samples in supercooled liquid helium or liquid nitrogen, respectively, in an immersion cryostat described previously [5,6]. Intermediate temperatures were obtained using an air products cryotip with liquid helium as the cryogen. Fluorescence excitation was provided by 90° illumination with a 1600 W high pressure xenon arc lamp using a Jarrell–Ash 0.25 m monochromator and a 15 cm water cell as filters. Similarly, absorption illumination was provided with a 1600 W high pressure xenon arc lamp from behind the sample using $NiSO_4$ and $CoSO_4$ in water solution as a filter. The spectra were recorded photographically and photoelectrically on a Jarrell–Ash 1 m double Czerny–Turner spectrograph–spectrometer. The photon-counting photoelectric system allowed for digital recording of the data on magnetic tape and subsequent processing on an IBM 360 series computer [5].

2.1. Synopsis of theory

Because HMB is a neutral molecule forming a one-molecule-per-unit-cell molecular crystal, it can be adequately and easily treated with the Frenkel tight binding exciton theory. The general derivation for molecular crystals has been given elsewhere [1,6,7] and only those results related to this work will be given. The basic simplification in this treatment is indicated in the one site crystal wavefunction which is written as

$$\phi^0_{\eta'} = \mathcal{A}\,\chi^f_{\eta'} \prod_{\eta\neq\eta'}^{N} \chi^0_{\eta}, \tag{1}$$

where $\mathcal{A}$ is an antisymmetrizing operator (for electronic excited states) and $\chi^f_{\eta'}$ is the site adapted wavefunction of a molecule at the η'th site in the fth excited state. Note that there is no subscript α to designate the representation in the crystal's interchange group because that group is the trivial C_1. The theory then gives for the general κ-dependent matrix element for the fth excited state:

$$\mathcal{D}^f(\kappa) = \frac{1}{2N}\sum_{\eta=1}^{N}\sum_{l=1}^{N}(1-\delta_{\eta l})\exp[-i\kappa\cdot(R_\eta - R_l)] \times \int \phi^{f*}_{\eta} H'_{\eta\eta'} \phi^f_{\eta'}\,d\tau, \tag{2}$$

which is the dispersion relation giving the distribution of energy levels for the fth state as a function of κ. To evaluate $\mathcal{D}^f(\kappa)$, one must first evaluate the integral

$$M_{\eta\eta'} = \int \phi^{f*}_{\eta} H'_{\eta\eta'} \phi^f_{\eta'}\,d\tau. \tag{3}$$

The value of $M_{\eta\eta'}$ is best determined experimentally by recognizing that it is simply the pairwise interaction between a molecule at site η and another at site η', i.e., a dimer in the crystal. Since the first singlet transition is weak (forbidden in benzene [1] and allowed only due to the slight perturbation of the S_6 site [4]) the transition-dipole–transititon-dipole contributions are very small. Thus higher order contributions, like octopole–octopole or electron exchange integrals must dominate the pairwise exciton interactions, i.e. $M_{\eta\eta'}$ decreases rapidly as the intermolecular separation increases. Therefore it is a reasonable assumption to reduce the summation in eq. (2) to only a few terms, i.e.,

$$\mathcal{D}^f(\kappa) \approx P^{-1}\sum_{\eta=1}^{P} M_{0,\eta}\exp[i\kappa\cdot(R_0 - R_\eta)], \tag{4}$$

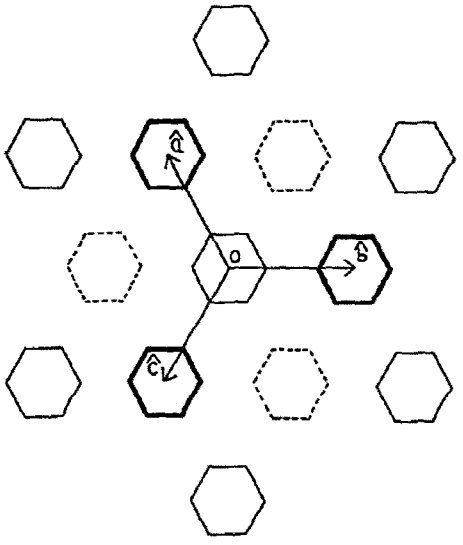

Fig. 1. Trigonal lattice with basis vectors. Three successive layers of molecules are seen in this view of the predicted phase III crystal structure of hexamethylbenzene. The benzene rings are oriented to give the maximum D_{3d} site symmetry and the methyl groups have been omitted. The true S_6 site symmetry is realized by consideration of the methyl group positions and/or a rotation of the benzene rings about their six-fold axes. The basis vectors extending from the origin molecule in the middle layer to the three out-of-plane nearest-neighbor molecules in an adjacent layer were chosen to simplify the exciton band dispersion relation, eq. (6).

where η goes over the P most significant near neighbors of the molecule at site 0. Eq. (4) is further simplified by the inversion symmetry of the molecular site to

$$\mathcal{L}^f(\kappa) \approx P^{-1} \sum_{\eta=1}^{P/2} 2M_{0,\eta} \cos[\kappa\cdot(R_0 - R_\eta)]. \qquad (5)$$

In the low temperature phase III of HMB, spectroscopic studies indicate that the crystal structure is trigonal and has a three-fold axis of rotation perpendicular to the molecular plane [4,6]. The set of basis axis vectors in the trigonal lattice chosen to evaluate $\mathcal{L}^f(\kappa)$ is illustrated in fig. 1 and is designated $\hat{a}$, $\hat{b}$, and $\hat{c}$. These basis vectors were chosen to give a simpler and more symmetric dispersion relation. The out-of-plane nearest neighbors from the origin molecule are at $\pm\hat{a}$, $\pm\hat{b}$, and $\pm\hat{c}$, the in-plane nearest neighbors are at $\pm(\hat{a}-\hat{b})$, $\pm(\hat{b}-\hat{c})$, and $\pm(\hat{c}-\hat{a})$. Two further sets of out-of-plane near neighbors also included are those at $\pm(\hat{a}+\hat{b})$, $\pm(\hat{b}+\hat{c})$, and $\pm(\hat{c}+\hat{a})$ and the two at $\pm(\hat{a}+\hat{b}+\hat{c})$. The resulting dispersion relation then becomes

$$\begin{aligned}\mathcal{L}^f(\kappa) \approx\ & 2M_{0,\hat{a}-\hat{b}}\{\cos[\kappa\cdot(\hat{a}-\hat{b})] \\ & + \cos[\kappa\cdot(\hat{b}-\hat{c})] + \cos[\kappa\cdot(\hat{c}-\hat{a})]\} \\ & + 2M_{0,\hat{a}}(\cos\kappa\cdot\hat{a} + \cos\kappa\cdot\hat{b} + \cos\kappa\cdot\hat{c}) \\ & + 2M_{0,\hat{a}+\hat{b}}\{\cos[\kappa\cdot(\hat{a}+\hat{b})] + \cos[\kappa\cdot(\hat{b}+\hat{c})] \\ & + \cos[\kappa\cdot(\hat{c}+\hat{a})]\} + 2M_{0,\hat{a}+\hat{b}+\hat{c}}\cos[\kappa\cdot(\hat{a}+\hat{b}+\hat{c})], \qquad (6)\end{aligned}$$

where the effect of the three fold site symmetry on the $M_{0,\eta}$ is considered. The dispersion relation is then easily evaluated by computer over the first Brillouin zone of the reciprocal lattice space [7]. This gives the density of energy states $\rho(E)$ for the fth excited state, once the appropriate $M_{0,\eta}$ values are available.

To interpret properly the spectroscopic data obtained from experiment, it is necessary to investigate the nature of the selection rules for optical transitions in the crystal [8]. For a Frenkel exciton in a one-molecule-per-unit-cell crystal, the transition dipole operator is simply the sum of the transition dipole operators for all of the molecules in the crystal, i.e,,

$$M = \sum_{\eta=1}^{N} M_\eta. \qquad (7)$$

The transition dipole matrix element using the one site Frenkel exciton function for states f'' and f is

$$T = \langle\phi^{f''}(\kappa)|M|\phi^f(\kappa)\rangle. \qquad (8)$$

In expanding eq. (8), the wave vector of the incident radiation is assumed equal to zero and the orthogonality of the molecular wavefunctions is used to give

$$\begin{aligned}T = N^{-1} & \sum_{\eta=1}^{N} \exp(-i\kappa''\cdot R_\eta)\exp(i\kappa\cdot R_\eta) \\ & \times \int \phi_\eta^{f''*} M_\eta \phi_\eta^f \, d\tau. \qquad (9)\end{aligned}$$

The two exponential factors then reduce to a Kronecker delta function and eq. (9) becomes

$$T = N^{-1}\delta_{\kappa''\kappa} \sum_{\eta=1}^{N} \int \phi_\eta^{f''*} M_\eta \phi_\eta^f \, d\tau, \qquad (10)$$

which illustrates two important selection rules for Frenkel excitons. First, the transition will be allowed only if $\Delta\kappa = 0$ (from the $\delta_{\kappa''\kappa}$). As a further consequence of this factor in eq. (10), note that the magnitude of the transition dipole is κ-independent. Second, if one

of the two states, f'' or f, is the ground state (which is totally symmetric and for which the only κ value is zero) then the only observable transition to or from the ground state involves a $\kappa = 0$ state [6]. We notice that in the general case, that of non-trivial interchange symmetry, eq. (10) can be derived only in the limit of the *restricted* Frenkel exciton [8] (i.e. neglecting certain next-nearest pairwise interactions). However, no such approximation is necessary in our present case of only one molecule per primitive unit cell.

3. Results

The absorption spectrum ($^1A_u \leftarrow {}^1A_g$) of a thin crystal ($\approx 10\,\mu$) of neat HMB at 2 K is shown in fig. 2. The single sharp absorption peak at 35134 cm^{-1} is the allowed $\kappa = 0$ transition to the ^1A_u first excited singlet state of HMB crystal [9]. The absorption spectrum in fig. 3 is again of the singlet origin of HMB, but in this case for the dilute (0.6% mole) isotopic guest in a host crystal of HMB-d_{18}. The sharp absorption peak at 35156 cm^{-1} is the origin of the monomer spectrum of HMB in the isotopic host as opposed to the $\kappa = 0$ allowed origin of crystalline neat HMB [6,10]. To a first approximation the monomer origin is also the center of gravity of the exciton band. Hence, an approximate width of the exciton band is immediately determined as twice the energy difference between the $\kappa = 0$ and monomer origins; i.e., about 44 cm^{-1}. This is a good approximation providing the exciton band density of states is reasonably

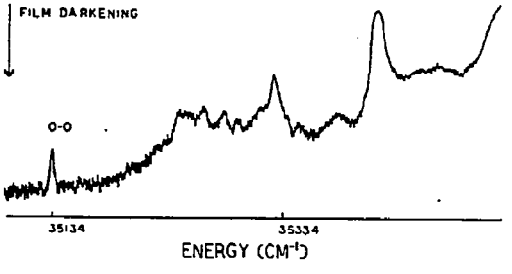

Fig. 2. Absorption origin of hexamethylbenzene at 2 K. The single $\kappa = 0$ component of the first excited singlet exciton band of hexamethylbenzene is observed at 35134 cm^{-1} in the 2 K absorption spectrum of a thin ($\approx 10\,\mu$) crystal of hexamethylbenzene. The half-width at half height is 4 cm^{-1}.

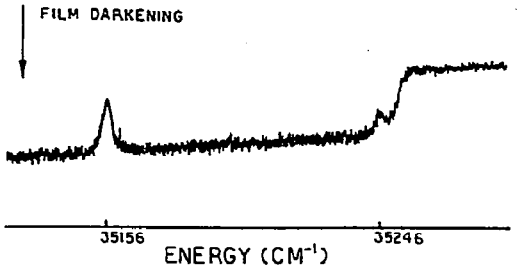

Fig. 3. Absorption origin of 0.6 mole percent hexamethylbenzene at 2 K. The origin of the monomer hexamethylbenzene species' first excited singlet state is observed at 35156 cm^{-1} in the absorption spectrum of a 0.6 mole percent hexamethylbenzene in perdeuterohexamethylbenzene crystal. The half-width at half height is 4 cm^{-1}.

symmetric and the $\kappa = 0$ state does lie at the bottom of the band and assuming a negligible D term change with isotopic substitution and a small quasiresonance shift [11].

In order to investigate directly the exciton band, it is necessary to investigate an optical transition which does not involve the ground state; i.e., a transition must be observed involving two exciton bands which possess all the κ states of the crystal. A good representation of the exciton band density of states can be obtained from such a transition providing the exciton band of the state to be investigated is much wider in energy than the other state, usually a ground state vibration. The most direct way of observing an exciton band's density of states is in a hot-band absorption which has a ground state vibration as its origin and the electronic exciton band as its final state. This method is convenient since if the origin band is narrow, the relative population of states in the *vibrational* exciton band can be assumed to be constant at temperatures high enough to thermally populate the band so that it might be observed as an origin for a transition.

A hot-band absorption spectrum of HMB at 77 K is seen in fig. 4. The most intense feature in the hot-band spectrum is the $0' \leftarrow 454$ cm^{-1} transition and the least intense is the $0' \leftarrow 363$ cm^{-1} transition. The broad feature in the middle does not agree with any known Raman transition [6] but probably is a $0' \leftarrow 407$ cm^{-1} fundamental transition and in this experiment

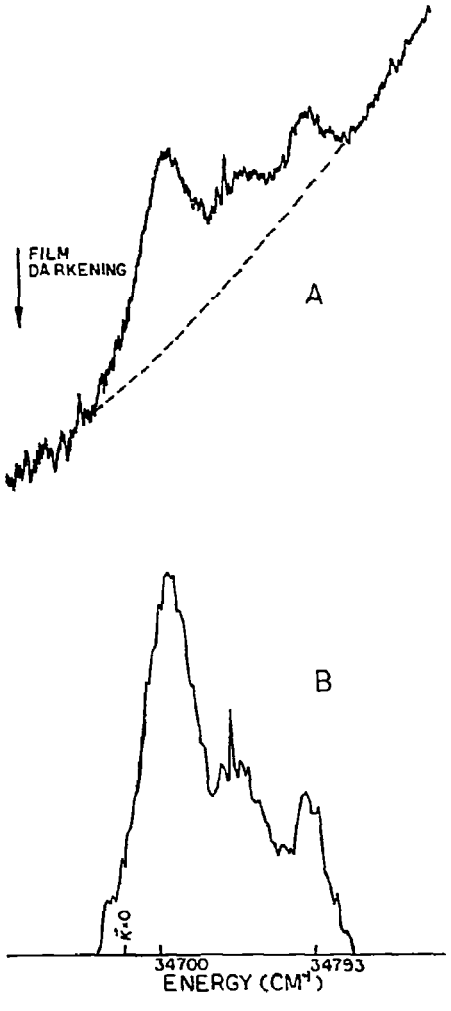

Fig. 4. Hot-band absorption of hexamethylbenzene. The hot-band transitions from three ground state fundamentals at 363 cm^{-1}, 407 cm^{-1}, and 454 cm^{-1} to the first excited singlet exciton band of hexamethylbenzene are observed in the 77 K absorption spectrum of a thick (≈ 2 mm) crystal of hexamethylbenzene. (A) is a microdensitometer trace of the three hot bands in the absorption spectrum. The dotted line is the extrapolated background. (B) is the three hot bands with the background intensity subtracted to show the true bandshapes. The $\kappa = 0$ state shown for the $0' \leftarrow 454$ cm^{-1} transition is determined by shifting the singlet $\kappa = 0$ state at 35134 cm^{-1} by –454 cm^{-1}.

it is masking part of the exciton density of states in the other two fundamental transitions and probably broadens the $0' \leftarrow 454$ cm^{-1} transition to higher energy.

Even though the $0' \leftarrow 454$ cm^{-1} transition cannot give the full density of states, several aspects of the exciton band are now known from this transition. By comparing the displacement (Raman) [6] of the 454 cm^{-1} vibration from the known $\kappa = 0$ and monomer energies with the $0' \leftarrow 454$ cm^{-1} hot band, it is seen that one, the $\kappa = 0$ state does lie near the bottom of the band and two, the 44 cm^{-1} estimate of the band width is not an unreasonable value.

The alternative experiment to the hot-band absorption for investigation of the exciton band density of states is the temperature dependent neat crystal fluorescence. Although the neat crystal fluorescence of HMB is very weak and this experiment requires good temperature control and a subsequent Boltzmann temperature correction, it is advantageous over the hot-band absorption in that selection of the most favorable transition is possible rather than being restricted to those which are sufficiently thermally populated for the transition to occur. It is also true that the exciton band density of states determinations of benzene and naphthalene were done primarily from fluorescence studies [1,2].

The $0' \leftarrow 454$ cm^{-1} transition was selected for the exciton band determination because of its relative intensity and its isolation from other transitions. The transition and its necessary corrections are shown in fig. 5. Inasmuch as the signal at the desired resolution was weak, the spectra were scanned eight times with the data being collected digitally on magnetic tape. The data were then calibrated and concatenated on a computer to give the resulting spectra in fig. 5b. A point by point correction for the Boltzmann temperature distribution at 30 K (the experimental temperature) gave the "experimental exciton density of states" shown in fig. 5c.

In order to compare the experimental density of states with the previously mentioned data, the $\kappa = 0$ energy displaced by –454 cm^{-1} and the center of the band (mean energy) are also displayed in fig. 5c. As in the absorption spectrum in fig. 4b, the $\kappa = 0$ state is observed to lie very close to the bottom of the band. The center of the band was compared to the $0' \rightarrow 454$ cm^{-1} transition in a 1% HMB in HMB-d_{18} isotopic mixed crystal at 30 K and is found to agree with the monomer energy to within 1 cm^{-1} [6].

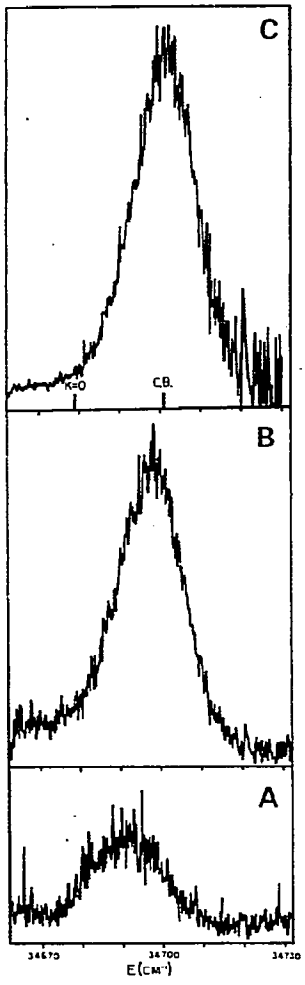

Fig. 5. Determination of the exciton band density of states from the $0' \rightarrow 454$ cm^{-1} fluorescence of hexamethylbenzene. The three basic steps in the experimental determination of the density of states of the first excited singlet state of hexamethylbenzene are illustrated. (A) is the fluorescence spectrum of the $0' \rightarrow 454$ cm^{-1} band of a neat hexamethylbenzene crystal at 30 K recorded on nine-track magnetic tape by photon counting methods. The spectrum is calibrated and plotted by computer and the calibrated data is stored on magnetic tape. This spectrum was repeated eight times. (B) is the eight individual spectra concatenated into one spectrum to improve the signal to noise ratio. In (C) a Boltzmann temperature correction was applied to each point in the concatenated spectrum (B) after correcting for the non-zero baseline. The resultant band is the experimentally determined exciton band density of states for the first excited singlet state of hexamethylbenzene. The $\kappa = 0$ state is determined by shifting the singlet $\kappa = 0$ state at 35134 cm^{-1} by -454 cm^{-1}. The center of band (CB) is determined by numerically integrating to one half the intensity of the band.

4. Discussion

The experimentally determined density of states for the first excited singlet exciton band of HMB is quite accurate as the data was collected in digital form by photon counting, thus bypassing the difficulty of calibrating a photographic plate and also being able to process the data easily and accurately on a computer. The digital form of the data also facilitates a simpler form of data storage and transport as well as simplifying comparison of experiment to theory.

Now that the experimental density of states of the singlet exciton band of HMB is known, the problem remains to test its agreement with the Frenkel exciton theory by comparison with a calculated density of states. The general procedure is to calculate the band's energy states as a function of κ using the dispersion relation [eq. (6)] and counting the number of states in each increment of energy. The $M_{0,\eta}$ values are usually determined [12] by measuring the energy shifts of dimer states in dilute isotopic mixed crystals. However, in the case of HMB, it has not been possible to resolve any dimer states for two reasons. First, as will be shown later, the dimer energies are probably displaced by less than 4 cm^{-1}. This should not be a problem since the resolution of the experiment is 1 cm^{-1}, except for the second reason, that the best resolved monomer absorption band has a half-width of 4 cm^{-1}. These two facts combined with the topology of the crystal give a monomer and at least two dimer states, each with an expected half-width of 4 cm^{-1}, in a 4 cm^{-1} spectral region. Thus it has not been possible to use dimer states to predict $M_{0,\eta}$ values to calculate a Frenkel exciton band. But it has been possible to use the available data and calculate the exciton band by a band fitting procedure and thereby arrive at reasonable $M_{0,\eta}$ values.

In order to examine the behavior of the Frenkel exciton band as a function of the $M_{0,\eta}$ values, the dispersion relation was truncated to include only the nearest or immediately adjacent neighbors; i.e., set $M_{0,\hat{a}+\hat{b}}$ and $M_{0,\hat{a}+\hat{b}+\hat{c}}$ equal to zero. Then the $\kappa = 0$ shift is

$$\mathcal{L}(\kappa = 0) = 6M_{0,\hat{a}-\hat{b}} + 6M_{0,\hat{a}} = -22 \text{ cm}^{-1}, \qquad (11)$$

where -22 cm^{-1} is the energy displacement from the center of the band to the $\kappa = 0$ state. Within the restriction of eq. (11), a set of sample Frenkel exciton

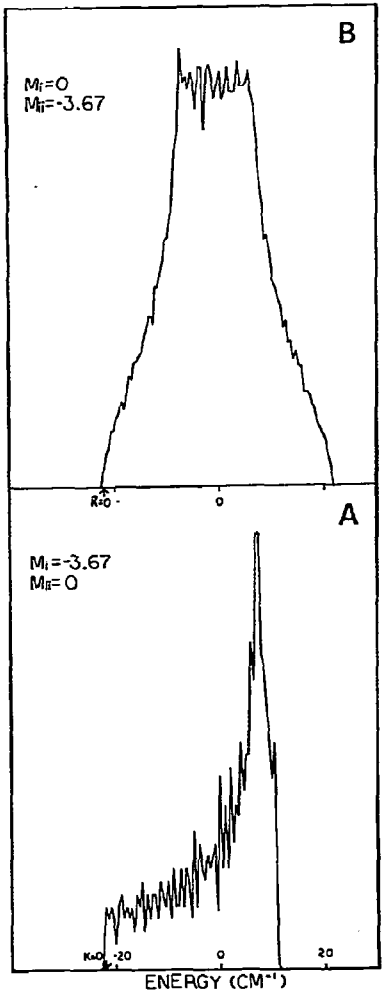

Fig. 6. Frenkel exciton bands calculated for hexamethylbenzene with one set of equivalent pairwise interactions. Two Frenkel exciton bands were calculated for hexamethylbenzene to examine the effect of the in-plane versus out-of-plane nearest-neighbor pairwise interactions. Each band was calculated with the dispersion relation [eq. (6)], setting one of the nearest-neighbor interaction parameters equal to -3.67 cm^{-1} and the other equal to 0.0 cm^{-1}. The in-plane interaction results in the asymmetric bandshape in (A) due to the sine terms in the dispersion relation. The out-of-plane interaction results in a very symmetric bandshape in (B) because it has only cosine terms in the dispersion relation. The vertical axes are in number of states. Each band was calculated over a lattice of 125000 molecules.

bands can be calculated and compared to experiment to check if limits can be assigned to the $M_{0,\eta}$'s.

A first step is to put one of the $M_{0,\eta}$ values equal to zero and see what the effect on the band is with the total intermolecular interaction either in-plane or out-of-plane. These two bands are displayed in fig. 6. The in-plane interaction band in fig. 6a is characterized by a very asymmetrical shape which is strongly peaked to high energy. While the $\kappa = 0$ lies at the bottom of the band, a visual comparison quickly shows a poor agreement in bandshape with the experimental band. The high degree of asymmetry is due to the sine terms in the in-plane terms of the dispersion relation. The out-of-plane band in fig. 6b is much more symmetric in shape with the $\kappa = 0$ again at the bottom of the band. This is expected because the out-of-plane terms in the truncated dispersion relation have only cosine terms, which are symmetric in the $-\pi$ to π interval over which the band calculation is done. It can be assumed at this point that the dominant interaction in the exciton band is probably the out-of-plane intermolecular interaction.

The next step is to calculate exciton bands for a range of values of $M_{0,\hat{a}}$ and $M_{0,\hat{a}-\hat{b}}$ utilizing eq. (11) to relate the values to the $\kappa = 0$ shift. A series of such bands is displayed in fig. 7 where $M_{0,\hat{a}}$ has been assigned values from -5.6 cm^{-1} to -0.8 cm^{-1}. These calculated bands span the extremes of bandshape between which the experimental case is assumed to lie. At one extreme, for $M_{0,\hat{a}} < -4.0$ cm^{-1}, the calculations demonstrate a rapidly growing bandwidth and a steeply rising low energy band edge. The band for which $M_{0,\hat{a}} = -4$ cm^{-1} is in agreement with the experimental data for the bandwidth and the high energy side of the band, but the low energy side of the experimental band is more asymmetric than this calculated band. In the other extreme, for $M_{0,\hat{a}} > -3.0$ cm^{-1}, the calculated bandwidth decreases and becomes sharply peaked at high energy. At $M_{0,\hat{a}} = -3$ cm^{-1}, the low energy band edge is in good agreement with the experimental data but the high energy side deviates sharply. Thus, the value of $M_{0,\hat{a}}$ is probably between -3.0 and -4.0 cm^{-1} and $M_{0,\hat{a}-\hat{b}}$ is between -0.67 and 0.10 cm^{-1} for the truncated dispersion relation with two parameters. It is also evident that the asymmetry of the band is due to the in-plane parameters.

The two-parameter exciton band calculation can be optimized to the experimental data by slowly varying $M_{0,\hat{a}}$ between -3.0 and -4.0 cm^{-1} and comparing

the experimental band to the calculated bands after normalizing the bands to a common area. The best fit is found for values of $M_{0,\hat{a}}$ equal to -3.0 to -3.3.

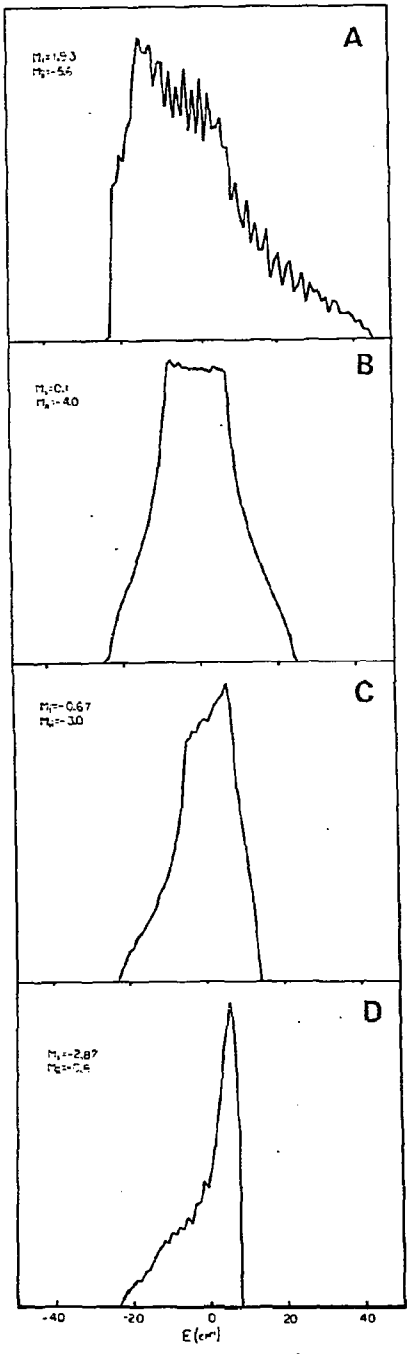

cm^{-1}. The lower energy side of the band fits very well and most of the variation is found in the high energy side of the band (see fig. 8). The sharp maximum of either band cannot be fitted to the experimental data and the total bandwidth is more in agreement with $M_{0,\hat{a}}$ equal to -3.3 cm^{-1}. Thus the two-parameter band indicates that the out-of-plane interaction is about -3.3 cm^{-1} and the in-plane interaction is about -0.4 cm^{-1}.

Similar calculations were attempted with the four-parameter dispersion relation [eq. (6)] but were unproductive in that a suitable potential function could not be obtained to relate the four parameters: A transition-octopole–transition-octopole [9b] potential function was tried without success [6]. This is not surprising [12b]. Actually, the nearest-neighbor out-of-plane interaction is probably due to $\pi-\sigma$ interactions [13], i.e. methyl groups interacting with the ring π-electrons rather than an interaction between the two-ring π-electron systems. Furthermore, the terms due to the other two parameters would only contribute to the asymmetry of the band as with the in-plane interaction and thus would probably have very small values.

The two-parameter dispersion relation

$$\mathcal{L}^f(\boldsymbol{\kappa}) \approx 2M_{0,\hat{a}-\hat{b}}\{\cos[\boldsymbol{\kappa}\cdot(\hat{a}-\hat{b})] + \cos[\boldsymbol{\kappa}\cdot(\hat{b}-\hat{c})] + \cos[\boldsymbol{\kappa}\cdot(\hat{c}-\hat{a})]\} + 2M_{0,\hat{a}}(\cos\boldsymbol{\kappa}\cdot\hat{a} + \cos\boldsymbol{\kappa}\cdot\hat{b} + \cos\boldsymbol{\kappa}\cdot\hat{c}) \qquad (12)$$

appears to be sufficient to fit the experimental data. If the dispersion relation is calculated for $\boldsymbol{\kappa}$ along the C_3 axis (in reciprocal space) of the site group (fig. 9), it is seen that the upper and lower energy limits of the band are defined by $\boldsymbol{\kappa} = \pm\pi$ and $\boldsymbol{\kappa} = 0$, respectively.

Fig. 7. Frenkel exciton bands calculated for hexamethylbenzene with two sets of equivalent pairwise interactions. Four Frenkel exciton bands calculated from the dispersion relation (6) using the two nearest-neighbor pairwise interaction $M_{\hat{a}}$ and $M_{\hat{a}-\hat{b}}$ illustrate the extremes in bandshape between which the best fit to the experimental exciton density of states for hexamethylbenzene is found. The pairwise interactions are: (A) $M_{\hat{a}} = -5.6$ cm^{-1}, $M_{\hat{a}-\hat{b}} = 1.93$ cm^{-1}; (B) $M_{\hat{a}} = -4.0$ cm^{-1}, $M_{\hat{a}-\hat{b}} = -0.1$ cm^{-1}; (C) $M_{\hat{a}} = -3.0$ cm^{-1}, $M_{\hat{a}-\hat{b}} = -0.67$ cm^{-1}; (D) $M_{\hat{a}} = -0.8$ cm^{-1}, $M_{\hat{a}-\hat{b}} = -2.87$ cm^{-1}. The vertical axes are in number of states. Each band was calculated over a lattice of at least 125000 molecules.

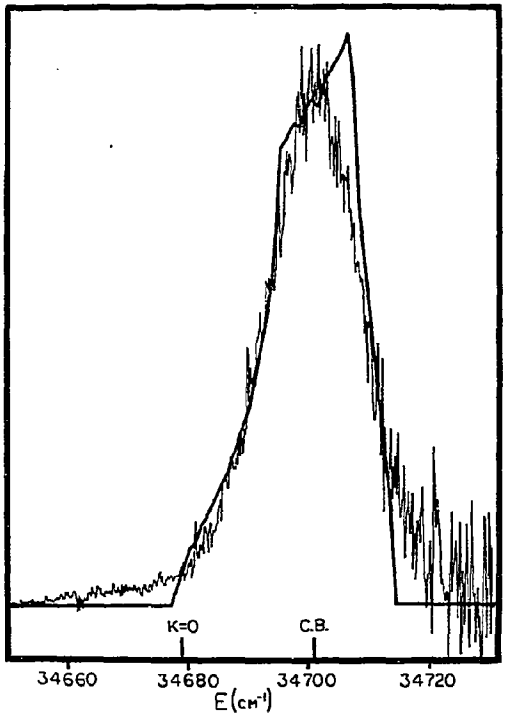

Fig. 8. Frenkel exciton band calculated for hexamethylbenzene with two sets of equivalent pairwise interactions and fit to the experimental density of states. The two nearest-neighbor pairwise interactions were optimized to calculate the Frenkel exciton band which would best fit the experimental density of states determined for hexamethylbenzene. The interaction parameters were $M_{0,\hat{a}} = -3.3$ cm^{-1} and $M_{0,\hat{a}-\hat{b}} = -0.4$ cm^{-1} to give a calculated $\kappa = 0$ shift of -22 cm^{-1}. The calculated and experimental densities of states are superimposed to show the extent to which they agree. The $\kappa = 0$ state and the center of band (CB) correlate to $\pm$ 1 cm^{-1}. The vertical axis is the number of states. The theoretical band was calculated for a lattice of 125000 molecules.

The $M_{0,\eta}$'s determined from the calculated band fitting also prove to be consistent with the isotopic mixed crystal absorption spectra for HMB shown in fig. 10. Using the S_6 topology of the site and accounting for the twelve nearest neighbors, the 3% HMB origin band can be easily calculated using lorentzian bandshapes for each of the components [6], as shown in fig. 11. The resultant spectrum shows the asymmetric broadening of the origin due to the nonresolvable dimers and agrees well with the experimental spectrum (fig. 10). Similar calculations for the 10% HMB origin band were too tedious because of the

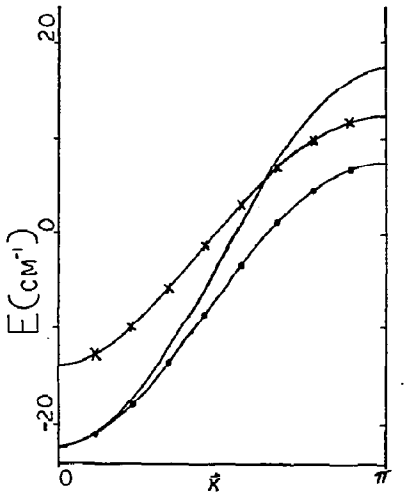

Fig. 9. The dispersion relation [eq. (12)], calculated along several directions in the first Brillouin zone of HMB: —— C_3 axis, $\kappa_a = \kappa_b = \kappa_c$; –•– C_2'' (in D_{6h}) axis, $\kappa_a = -\kappa_b$, $\kappa_c = 0$; –x– $\kappa_a = -\kappa_b$, $\kappa_c = \pi/2$.

large number of different configurations of N-mer clusters with the twelve nearest neighbors. However, an attempt to estimate the shape of the 10% HMB origin band showed good consistency with the experimental data. The data in table 1 shows the percentages of N-mers for different concentrations of HMB isotopic mixed crystals. It is seen there that $\approx$ 50% of the HMB molecules in a 10% isotopic mixed crystal exist in N-mers where N is four or more while the relative amount of each of those N-mers is probably less than 5%, with many configurations for each N-mer. Hence many reasonably large N-mers or clusters of HMB will be expected. Representative calculations on some of the larger N-mers then give some idea of the expected distribution of states in the absorption band. Linear N-mers, of which only a small percentage will be expected, will have their strongest absorption transitions converge on $-2M_{0,\eta}$ as N gets large. However, for N-mers where the molecules are tightly grouped, the strongest transition exceeds $-2M_{0,\hat{a}}$ or -6.6 cm^{-1}. For example, calculations for tightly grouped heptamers give absorption transitions at ≈ -8 cm^{-1}, which is in agreement with the partially resolved splitting seen in the 10% HMB absorption origin. If reasonable assumptions are made concerning the distribution of N-mers from table 1,

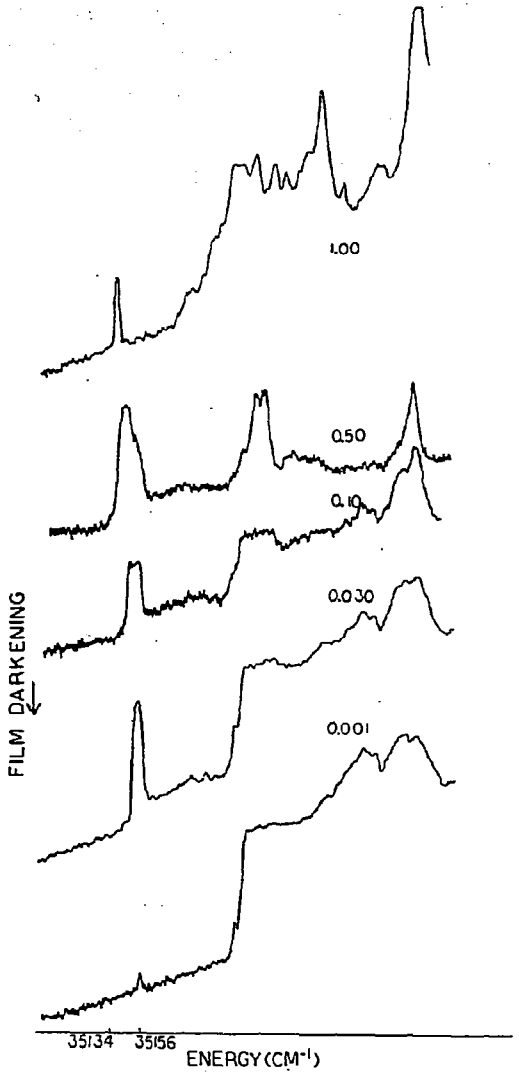

Fig. 10. Electronic singlet absorption spectra of hexamethylbenzene in different concentrations of isotopically mixed crystals. The absorption spectra of the singlet origin of hexamethylbenzene in several concentrations of isotopically mixed hexamethylbenzene crystals at 2 K are presented. The concentrations in the figure are mole percent hexamethylbenzene in perdeuterohexamethylbenzene. The spectral resolution is $\approx 1\ cm^{-1}$.

then the 10% HMB absorption origin is simply seen to be the absorption of a large number of assorted N-mers with the higher energy, partially resolved, component being primarily due to the $\approx 30\%$ monomer species and the lower energy component due to large,

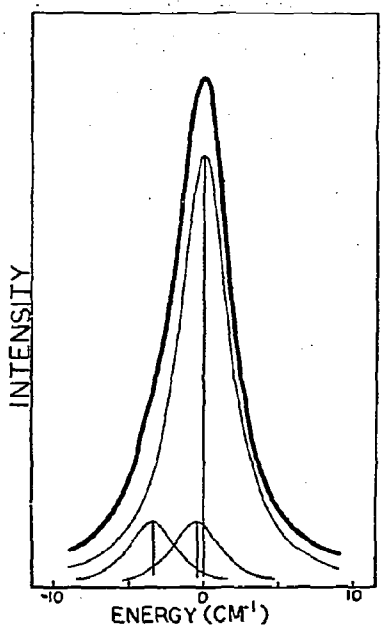

Fig. 11. Calculated absorption spectrum of the hexamethylbenzene singlet origin in a 3.0 mole percent isotopic mixed crystal. The absorption spectrum of the singlet origin of a 3.0 mole percent isotopic mixed crystal of hexamethylbenzene was calculated using lorentzian bandshapes for the significant components in the origin. The intensities of the components are in proportion to their probability of occurrence as calculated from a model with S_6 site symmetry and two sets of six equivalent nearest neighbors (table 1). Thus the only significant contributions to the origin band were found to be the monomer and dimer species. The component half-width at half-height values were taken to be 4 cm^{-1}, the minimum observed for a hexamethylbenzene transition, and the splitting terms for the dimers were taken from the exciton band parameters (-3.3 and $-0.4\ cm^{-1}$).

Table 1
Distribution of N-mers in isotopically mixed crystals of hexamethylbenzene [a]

N-mer	Percent of isotopic guest in crystal		
	0.1%	3.0%	10.0%
monomer	98.8%	69.4%	28.2%
dimer	1.18%	20.8%	18.0%
trimer	0.005%	2.4%	4.6%
$N \geq 4$	0.015%	7.4%	49.2%

[a] Expressed as percentage of the isotopic guest.

tightly grouped N-mers, with everything else contributing to the intensity in-between (cf. ref. [14]).

Another consequence of the S_6 site topology and the twelve nearest neighbors is seen in the fluorescence [6,10] of isotopic mixed crystals of HMB at 2 K. The energy of the fluorescence origin of HMB versus the square root of the guest concentration is seen in fig. 12. The linearity from 10 to 100% HMB concentration is expected from the separated band limit expression [15]

$$\tilde{Y}_g = C_g^{1/2} Y_g^0, \tag{13}$$

where $\tilde{Y}_g$ is the guest bandwidth, C_g is the guest concentration and $\tilde{Y}_g^0$ is the guest's neat crystal bandwidth. Since the origins plotted here come from the clusters with the lowest energy level available to the guest HMB exciton, this data implies that, at 10% HMB,

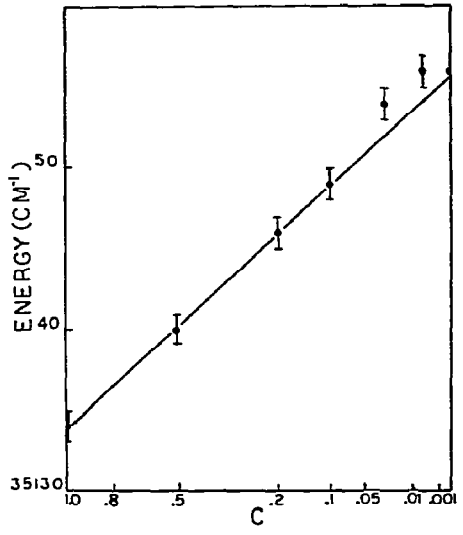

Fig. 12. Concentration dependence of the guest exciton band edge in isotopic mixed crystals of hexamethylbenzene. The lower energy edge of the guest singlet exciton band of isotopic mixed crystals of hexamethylbenzene in perdeuterohexamethylbenzene is plotted versus the square root of the concentration of the guest hexamethylbenzene. The band edge was determined [16] from absorption and fluorescence spectra of isotopic mixed crystals at the several concentrations. The straight line through the data points is predicted by eq. (13). The 0.0 concentration data point is the monomer energy predicted from the 0.6 and 0.1 mole percent isotopic mixed crystal data. Note that the 1 and 3 mole percent points are not expected to obey eq. (13), as these samples are definitely below the effective (dynamic) percolation concentration [17,18].

energy transfer in the crystal is efficient enough for the singlet exciton to "percolate" through the crystal and find the lowest energy site [16–18]. This is, for HMB, a direct consequence of the topology of the crystal since it can be easily demonstrated that with twelve nearest neighbors and with S_6 site symmetry, only about 1% of the *guest* molecules in a 10% HMB in HMB-d_{18} isotopic mixed crystal are isolated from other guest molecules by two or more host molecules. Within the lifetime of the singlet state, it is relatively easy for the exciton to jump (or tunnel) [17] across a single host molecule and "percolate" through the crystal [18] to find the lowest energy site from which to emit (and thus contribute to the band picture). This efficient energy transport is again consistent with having a relatively wide exciton band.

Similarly, the band picture can be tested by investigating the absorption spectral bandwidth as suggested by the separated band limit equation:

$$Y_g = (C_A C_B \mu_2^0)^{1/2}, \tag{14}$$

where we take Y_g as the full-width at half height of the spectral density, C_A and C_B are the concentrations of the guest and host species and μ_2^0 is the second moment of the guest's neat crystal exciton band [15]. The data displayed in fig. 13 again show reasonable agreement with what is predicted for the band behaviour in a heavily doped isotopic mixed crystal in the *separated band limit*. While this theoretical

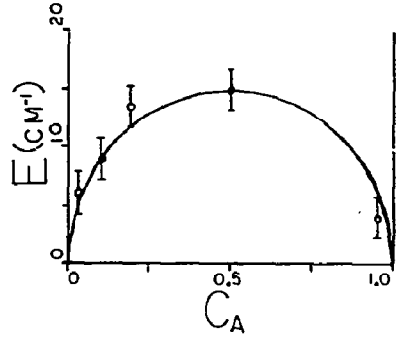

Fig. 13. Spectral widths of the origin absorption bands of several concentrations of HMB in HMB-d_{18} isotopic mixed crystals, plotted versus the HMB concentration. The solid line is the theoretical spectral half-width calculated from eq. (14), normalized for the 0.5 mole fraction HMB half-width. The "natural" linewidth of 4 cm^{-1} (as measured for both the pure crystal and the 0.1% sample) has been subtracted from all fwhh values.

formulation applies strictly only to energy bands above the cluster eigenstate percolation concentration [15,17a] (which should be somewhere between 0.2 and 0.3 mole fraction) the above mentioned behaviour of the cluster spectra (figs. 10 and 11) explains the reasonably good fit shown also by the lower concentration data points in fig. 13.

All our data are thus consistent with an exciton band that is an order of magnitude wider than previously expected [9b]. This again demonstrates the utility of adding heavily doped isotopic mixed crystal data as well as interband transition data to the traditional "Davydov splitting" data.

5. Conclusions

The exciton band density of states for the first excited singlet state of HMB was determined experimentally. The center of band is at 35156 cm^{-1} and the $\kappa = 0$ is at 35134 cm^{-1}. The full width of the band is about 40 cm^{-1}. By fitting the experimental band it was determined that the dominant pairwise interaction is the out-of-plane nearest-neighbor one with a value of about -3.3 cm^{-1}. The in-plane nearest-neighbor interaction has a value of about -0.4 cm^{-1}. Overall, the Frenkel exciton model is consistent with the experimental data, but a transition-multipole–transition-multipole expansion is not. Simple mixed crystal theory, and, in particular, the "separated band" model, agree well with experiment above the percolation concentration. Cluster-to-cluster energy transfer occurs at relatively low guest concentrations.

References

[1] S.D. Colson, D.M. Hanson, R. Kopelman and G.W. Robinson, J. Chem. Phys. 48 (1968) 2215.
[2] S.D. Colson and T.L. Netzel, J. Chem. Phys. 59 (1973) 3107.
[3] R. Kopelman, J. Chem. Phys. 47 (1967) 2631.
[4] S.D. Woodruff and R. Kopelman, J. Cryst. Molec. Struct., to be published.
[5] F.W. Ochs and R. Kopelman, Appl. Spectry. 30 (1976) 306.
[6] S.D. Woodruff, Ph.D. Thesis, The University of Michigan (1976).
[7] A.S. Davydov, Theory of molecular excitons (Plenum Press, New York, 1971).
[8] S.D. Colson, R. Kopelman and G.W. Robinson, J. Chem. Phys. 47 (1967) 27, 5462.
[9] (a) H.C. Wolf, Z. Naturforsch. 13a (1958) 336; Solid State Phys. 9 (1959) 1.
(b) O. Schnepp, J. Chem. Phys. 29 (1958) 56; 30 (1959) 48; Ann. Rev. Phys. Chem. 14 (1963) 35;
O. Schnepp and D.S. McClure, J. Chem. Phys. 26 (1957) 83.
[10] S.D. Woodruff, P.N. Prasad and R. Kopelman, J. Chem. Phys. 60 (1974) 2365.
[11] (a) G.C. Nieman and G.W. Robinson, J. Chem. Phys. 39 (1963) 1298;
(b) D.M. Hanson, R. Kopelman and G.W. Robinson, J. Chem. Phys. 51 (1969) 212.
[12] (a) D.M. Hanson, J. Chem. Phys. 52 (1970) 3409.
(b) H.-K. Hong and R. Kopelman, J. Chem. Phys. 55 (1971) 724.
[13] R. Kopelman, Record Chem. Progr. 31 (1970) 21.
[14] J. Hoshen and R. Kopelman, Phys. Stat. Sol. B, to be published.
[15] R. Kopelman, in: Excited states, Vol. 2, ed. E.C. Lim (Academic Press, New York, 1975).
[16] J. Hoshen, R. Kopelman and E.M. Monberg, J. Stat. Phys., to be published.
[17] (a) H.-K. Hong and R. Kopelman, J. Chem. Phys. 55 (1971) 5380;
(b) R. Kopelman, E.M. Monberg and F.W. Ochs, Chem. Phys. 19 (1977) 413; Topics in Appl. Phys., vol. 15.
[18] R. Kopelman, in: Radiationless processes in molecules and condensed phases, ed. F.K. Fong (Springer, Berlin, 1976).